Research Square

Preprints are preliminary reports that have not undergone peer review.
They should not be considered conclusive, used to inform clinical practice,
or referenced by the media as validated information.

Anatomy-Aware Regression Modeling of Distal Radius Morphology for Surgical Planning

Yuichi Yoshii

yyoshii@tokyo-med.ac.jp

Tokyo Medical University Ibaraki Medical Center

Yusuke Eda

University of Tsukuba Hospital

Tomohiko Inomoto

Tokyo Medical University Ibaraki Medical Center

Reo Asai

Tsukuba University Hospital Mito Clinical Education and Training Center, Mito Kyodo General Hospital

Yasukazu Totoki

University of Tsukuba Hospital

Akira Ikumi

University of Tsukuba Hospital

Takeshi Ogawa

NHO, Mito Medical Center Hospital

Research Article

Keywords: Regression model, Distal radius, Computed tomography, Three-dimensional

Posted Date: June 14th, 2026

DOI: https://doi.org/10.21203/rs.3.rs-9829815/v1

License: This work is licensed under a Creative Commons Attribution 4.0 International License.
Read Full License

Additional Declarations: No competing interests reported.

Abstract

Background: The distal radius has a complex three-dimensional structure that is not fully captured by conventional two-dimensional radiographic parameters. Simple geometric predictors of distal radius morphology may improve surgical planning and implant design. This study aimed to develop regression models that estimate linear distance (LD), vertical distance (VD), and palmar tilt (PT) using transverse diameter and normalized relative positions.

Methods: Computed tomography datasets from 105 normal wrists (53 males, 52 females) were analyzed. A 3D coordinate system was defined using the radius long axis. The transverse diameter (x) was measured in the coronal plane, and relative position (p; 0 = radial margin, 1 = ulnar margin) was defined along this diameter. At 3-mm sagittal intervals, LD, VD, and PT were recorded. LD was defined as the 3D distance between dorsal and palmar articular edges; VD as the vertical distance between these edges projected onto the sagittal plane; and PT as the angle between the articular surface and a plane perpendicular to the long axis. Second-order polynomial regression models were constructed to predict LD, VD, and PT from x and p. Two models were developed: a sex-independent model and a simplified sex-adjusted model including sex as a fixed effect. Model performance was evaluated using R^2, RMSE, and MAE.

Results: Polynomial models accurately estimated LD ($R^2 = 0.913$) and VD ($R^2 = 0.914$). Sex adjustment modestly improved accuracy for LD ($R^2 = 0.917$) and VD ($R^2 = 0.918$). PT showed poor predictability in all models ($R^2 \leq 0.091$).

Conclusion: Anatomy-aware polynomial regression using transverse diameter and relative position reliably predicts LD and VD, with minor improvement from sex adjustment. PT requires additional geometric descriptors. This framework supports simplified, quantitative tools for individualized surgical planning and implant optimization.

Trial registration: Not applicable.

Background

Distal radius fractures are among the most common skeletal injuries, and precise morphological understanding of the distal radius is essential for anatomical reduction, implant design, and biomechanical analysis [1–4]. Conventional 2D parameters—such as palmar tilt, radial inclination, and ulnar variance—are limited in representing complex 3D anatomy [5, 6]. Recent advances in three-dimensional (3D) computed tomography (CT) and digital reconstruction techniques have substantially improved the ability to quantitatively characterize bone morphology [7-9]. Compared with conventional 2D imaging, 3D CT allows generation of anatomically accurate surface models that preserve spatial relationships between cortical and articular structures. Using segmentation and coordinate-based reconstruction, detailed metrics such as curvature, inclination, and torsional alignment can be obtained, providing a robust framework for analyzing inter-individual variability in distal radius anatomy [5, 10, 11].

It has been demonstrated that CT-based morphometry reveals significant differences in articular curvature and radial styloid orientation, even among healthy individuals [12]. Another study reported variability in volar curvature, sigmoid notch depth, and styloid projection, findings that correlate with differences in wrist kinematics [13]. Such anatomical diversity has important implications for implant design and surgical precision. Standard pre-contoured plates may not conform accurately to patient-specific morphology, potentially leading to malalignment or screw misplacement. In contrast, 3D CT–based morphometric data enable the development of patient-specific or population-optimized implants, enhancing fixation accuracy and improving clinical outcomes.

However, conventional polynomial regression or shape modeling approaches capture only global curvature and may fail to represent localized triangular features where the radial margin tapers and the central articular surface broadens. We hypothesized that a regression model incorporating relative position along the transverse diameter could more accurately describe the local geometric changes in the distal radius. The objective of this study was to develop and validate anatomy-aware regression models to estimate linear distance, sagittal vertical distance, and palmar tilt from transverse diameter and its normalized relative positions.

Methods

Study Design and Participants

This retrospective case-control study (Level III evidence) was conducted using computed tomography (CT) scans obtained for contralateral comparison in patients with unilateral wrist pathology. The study was performed in accordance with the Declaration of Helsinki and approved by the Institutional Review Board of Tokyo Medical University. Reporting followed the STROBE guidelines for observational research. Only unaffected wrists with no history or symptoms of trauma or deformity were included. The final cohort comprised 105 wrists (53 males, 52 females), age-matched (males: mean 56.3 years, range 20–95; females: mean 58.2 years, range 18–91). Exclusion criteria included traumatic arm injury, skeletal immaturity, and previous surgery. CT images were acquired with the forearm in neutral rotation, covering from the metacarpal base to approximately 13 cm proximal to the radiocarpal joint.

3D Reconstruction and Coordinate System Definition

Computer analyzing software (BoneSimulater, Orthree, Osaka, Japan) was used to analyze the 3D bone model of distal radius. After importing image data into the software, a 3D surface models of the distal radius were constructed with a surface construction algorithm. The coordinate system was defined based on the 3D data of the distal radius. The long axis of the radius was calculated from the 3D surface model of the distal radius. The software finds the proximal-to-distal center curve of the radius shaft by analyzing its cross sections in various locations. Thereafter, the software calculated the central point at each level from the surface data of the radial diaphysis, and the approximate straight line based on the central points was defined as the long axis. The long axis of the radius was defined as the y-axis, the proximal direction was defined as positive and the distal direction as negative. The z-axis was parallel to

the orthogonal projection of the line that initiated at the base on the sigmoid notch of distal radius and continued to the radial styloid process on the plane perpendicular to the y-axis. The radial direction of the z-axis was defined as positive, and the ulnar direction was defined as negative. The x-axis was defined to be perpendicular to the yz plane, and the palmar direction defined as positive and the dorsal direction defined as negative. The yz plane, xy plane, and xz plane were defined as the coronal plane, sagittal plane, and axial plane, respectively. The origin of the coordinates was defined as the intersection of the joint surface and the long axis of the radius. The transverse diameter (x) was measured as the vertical distance from the tip of the radial styloid to the ulnar margin in the coronal plane (Figure 1-a). A normalized relative position (p; radial margin = 0, ulnar margin = 1) was defined across the transverse diameter. Sagittal reference planes were created at 3-mm intervals, and coordinates of dorsal and palmar reference points at the edge of distal radius joint surface were recorded (Figure 1-b). At each position, the linear distance (LD, mm), vertical distance (VD, mm), and palmar tilt (PT, °) were measured.

Linear distance (LD, mm): direct 3D distance between dorsal and palmar articular reference points (Figure 2-c1). Vertical distance (VD, mm): distance between dorsal and palmar articular reference points on the x-axis (Figure 2-c2). Palmar tilt (PT, °): angle formed between the articular surface and a plane perpendicular to the radial long axis (Figure 2-c3).

Polynomial Regression Model

A second-order polynomial regression model was selected as a parametric approach because distal radius morphology changes smoothly along the transverse diameter, and quadratic functions provide sufficient flexibility to represent global curvature while maintaining model interpretability and avoiding overfitting. In addition, the interaction term (x·p) was included to account for geometric variations that depend on both transverse diameter and relative position, reflecting the anatomical asymmetry between the radial and ulnar margins. For each parameter (LD, VD, PT), second-order polynomial regression models were fitted using x, p, and their interaction. Two regression models were constructed:

1. **Base model (sex-independent):**

$$Y=\beta_0+\beta_1 \cdot x+\beta \cdot p+\beta_3 \cdot x^2+\beta_4 \cdot p^2+\beta_5 \cdot (x \cdot p)$$

2. **Sex-adjusted model:**

$$Y=\beta_0+\beta_1 \cdot x+\beta \cdot p+\beta_3 \cdot x^2+\beta_4 \cdot p^2+\beta_5 \cdot (x \cdot p)+\beta_6 \cdot Sex$$

Sex was incorporated into regression modeling as a binary numerical variable (Female = 0, Male = 1). This coding scheme enabled direct interpretation of the regression coefficient of the sex term as the mean difference between males and females, holding other predictors constant.

Statistical Analysis

All regression analyses were performed using Python (v3.11, Anaconda Distribution). Two polynomial regression models were constructed to estimate morphological parameters: (1) a sex-independent second-order polynomial model, and (2) a simplified sex-adjusted model in which sex (0 = female, 1 = male) was included as an additional fixed effect without interaction terms. Model fitting and evaluation were conducted using the scikit-learn library, and results were cross-verified in SPSS (v31.0, IBM Corp.). Model performance was assessed using the coefficient of determination (R^2), root mean square error (RMSE), and mean absolute error (MAE). Residual distributions were evaluated for normality using Q–Q plots and the Shapiro–Wilk test. A significance level of $p < 0.05$ was applied for all statistical assessments.

Results

Actual plots on 2D coordinates are shown in Figure 3. Three-dimensional plots for linear distance (LD), vertical distance (VD), and palmar tilt (PT) are shown in Figure 4. The performance of each regression model is summarized in Table 1.

Second-order polynomial regression using transverse width and normalized relative position demonstrated high predictive accuracy for LD. Including sex as an additional covariate resulted in a small but consistent improvement in model performance. The sex term indicated that male wrists exhibit slightly larger LD values than female wrists.

The polynomial model also predicted VD with sub-millimeter error, indicating that the x–p coordinate framework captures the overall curvature of the distal radial rim. Sex adjustment again improved the fit marginally, with males demonstrating greater VD on average, consistent with LD findings.

In contrast to LD and VD, polynomial regression showed poor explanatory ability for PT. The addition of the sex term did not meaningfully enhance the model. These findings suggest that PT depends on local 3D surface features that are not represented by transverse width and relative position alone.

Regression Equations

The final polynomial equations for LD, VD, and PT without sex adjustment are presented below:

$$LD = -17.123 + 1.3364 \cdot x + 27.4354 \cdot p - 0.02089 \cdot x^2 - 24.4777 \cdot p^2 + 0.3589 \cdot (x \cdot p)$$

$$VD = -14.600 + 1.136 \cdot x + 26.714 \cdot p - 0.0173 \cdot x^2 - 24.219 \cdot p^2 + 0.3784 \cdot (x \cdot p)$$

$$PT = -32.091 + 3.2974 \cdot x + 9.884 \cdot p - 0.0588 \cdot x^2 + 3.6896 \cdot p^2 - 0.7565 \cdot (x \cdot p)$$

The final polynomial equations for LD, VD, and PT with sex adjustment are presented below:

$$LD = -13.820 + 1.1413 \cdot x + 27.4392 \cdot p - 0.0189 \cdot x^2 - 24.4778 \cdot p^2 + 0.3589 \cdot (x \cdot p) + 0.6585 \cdot Sex$$

$$VD = -11.1944 + 0.9353 \cdot x + 26.7183 \cdot p - 0.01524 \cdot x^2 - 24.2192 \cdot p^2 + 0.3783 \cdot (x \cdot p) + 0.6789 \cdot Sex$$

$$PT = -35.5284 + 3.5004 \cdot x + 9.8796 \cdot p - 0.0608 \cdot x^2 + 3.6897 \cdot p^2 - 0.7565 \cdot (x \cdot p) - 0.6853 \cdot Sex$$

Overall, LD and VD can be accurately estimated from transverse diameter and normalized relative position, with minor yet consistent enhancement when incorporating sex. In contrast, PT exhibited minimal predictability, suggesting that volar inclination is governed by geometric characteristics not captured within the simplified x-p coordinate system.

Discussion

This study presents an anatomy-aware regression framework for distal radius morphology prediction. Incorporating relative position significantly improved accuracy compared to conventional polynomial models. The model captured localized morphological asymmetry between the radial and ulnar regions. Previous morphometric studies have demonstrated gender and population differences in distal radius geometry [14-17]. Our model provides a continuous function describing these variations quantitatively. Although prediction of palmar tilt remained less accurate, likely due to complex volar curvature [15, 18], this approach provides a foundation for personalized preoperative simulation and implant contouring. Anatomy-aware modeling improved representation of local triangular curvature and asymmetry between the radial and ulnar margins. Sex-specific differences—greater influence of relative position in females and diameter in males—reflect morphological diversity.

The present study demonstrated that distal radius morphology along the volar-dorsal rim can be effectively characterized using a simple coordinate system defined by transverse width and normalized relative position. Second-order polynomial regression models accurately predicted both linear distance and vertical distance, achieving sub-millimeter error. These findings suggest that much of the curvature of the distal articular rim is governed by smooth, continuous shape transitions that can be approximated by low-order geometry. Prior CT-based morphologic analyses have similarly reported that distal radius curvature varies predictably across the transverse plane, particularly along the volar ridge and sigmoid notch region [14, 19, 20]. The high accuracy observed in the present models is consistent with those prior observations and indicates that global geometric patterns are sufficiently captured by the x-p coordinate framework.

In contrast, palmar tilt (PT) was not predictable using the same polynomial structure. Unlike LD and VD, which reflect surface height relative to a reference plane, PT represents the local slope of the articular surface—a quantity influenced by subtle curvature changes and regional 3D topology. Previous research has shown that volar inclination varies considerably across small regions of the distal radius and is sensitive to local anatomical differences, trabecular orientation, and individual loading patterns [21, 22]. Such localized features are not captured by a 1-dimensional parameterization of the rim, which likely explains the poor explanatory power for PT observed in our study. This finding is consistent with 3D morphometric studies reporting that wrist alignment parameters—particularly palmar tilt—are highly

variable and require full 3D surface reconstruction or advanced modeling techniques for accurate estimation.

The sex-adjusted models further revealed that male wrists demonstrated slightly greater LD and VD than female wrists. This observation aligns with prior CT-based anatomical studies showing sex-related differences in distal radius dimensions, joint surface area, and cortical geometry [14–17]. Although the magnitude of the difference was modest, including sex as a fixed-effect covariate improved prediction accuracy for both LD and VD, supporting the idea that population-level morphological factors can refine anatomy-aware regression models.

An important implication of this study is that distal radius morphology can be partially reconstructed from minimal measurements, such as transverse width and normalized positional information. This offers potential utility for preoperative planning, implant design, and AI-based prediction systems. For example, previous work has incorporated parametric modeling and statistical shape analysis to generate patient-specific reconstructions from limited inputs [23–25]. Using this model, if the implant position relative to the distal radius can be predicted, the screw lengths for each screw hole can be calculated using the regression model (Figure 5). Our findings support the feasibility of simplified models for some anatomical parameters. While LD and VD appear amenable to such modeling approaches, PT likely requires incorporation of additional geometric features or higher-dimensional representations, such as principal curvature vectors, surface normals, or deep-learning–based 3D encodings.

The limitations of this study must also be acknowledged. First, the polynomial model is inherently constrained in its ability to represent highly localized curvature or anatomical irregularities, underscoring the poor performance for PT. Second, the coordinate system parameterizes the articular rim in a single dimension, which simplifies the complexity of the distal radius. Finally, although sex was incorporated, additional demographic or biomechanical factors—such as age, handedness, or occupation—may contribute to variations in articular morphology. Future work should explore nonlinear or machine-learning models, including spline-based regression, random forest, XGBoost, or neural surface reconstruction, to improve prediction of surface orientation parameters such as palmar tilt.

Despite these limitations, this study provides a robust demonstration that anatomy-aware polynomial regression can efficiently capture major geometric features of the distal radius with clinically meaningful accuracy. This modeling framework may serve as a foundation for future development of low-input prediction systems, automated preoperative planning tools, or integration into CT-based virtual simulation environments.

Conclusions

Anatomy-aware regression models incorporating transverse diameter and relative position accurately predict 3D morphology of the distal radius. These models may serve as quantitative tools for patient-specific surgical planning, fracture fixation, and implant design.

Abbreviations

2D: Two-dimensional

3D: Three-dimensional

AI: Artificial Intelligence

CT: Computed Tomography

LD: Linear Distance

MAE: Mean Absolute Error

PT: Palmar Tilt

Q–Q plot: Quantile–Quantile Plot

R^2: Coefficient of Determination

RMSE: Root Mean Square Error

STROBE: Strengthening the Reporting of Observational Studies in Epidemiology

VD: Vertical Distance

Declarations

Ethics approval and consent to participate: The study was conducted in accordance with the Declaration of Helsinki, and approved by the Institutional Review Board of Tokyo Medical University (protocol code T2022-0041 and date of approval, Dec 14th, 2022). As this was a retrospective study, the requirement for written informed consent was waived by the Institutional Review Board. Instead, an opt-out approach was used, and participants were provided with the opportunity to refuse participation through a publicly available notice.

Consent for publication: Written consent for publication was obtained from all study participants.

Availability of data and materials: The datasets used and/or analyzed during the present study are available from the corresponding author upon reasonable request.

Competing interests: No benefits in any form have been received or will be received from a commercial party directly or indirectly related to the subject of this article.

Funding: This study was supported by a Grant-in-Aid for Scientific Research (23K08618), Zimmer Biomet Holdings, Inc. and Terumo Life Science Foundation. These funds were not involved in data collection, data analysis, or the preparation or editing of the manuscript.

Acknowledgements: Not applicable.

Author's contributions: YY: research design, acquisition and analysis of data, and wrote the manuscript, YE: acquisition and analysis of data and revise the manuscript, TI: acquisition and analysis of data and revise the manuscript, RA: acquisition and analysis of data and revise the manuscript, YT: acquisition and analysis of data and revise the manuscript, AI: acquisition and analysis of data and wrote the manuscript, TO: acquisition and analysis of data and wrote the manuscript. All authors were fully involved in the study and approved the final version of this manuscript.

References

1. Chung KC, Spilson SV. The frequency and epidemiology of hand and forearm fractures in the United States. J Hand Surg Am. 2001;26(5):908-15. doi: 10.1053/jhsu.2001.26322.
2. Francis JL, Battle JM, Hardman J, Anakwe RE. Patterns of injury and treatment for distal radius fractures at a major trauma centre. Bone Jt Open. 2022;3(8):623-7. doi: 10.1302/2633-1462.38.BJO-2022-0027.R1.
3. Mauck BM, Swigler CW. Evidence-based review of distal radius fractures. Orthop Clin North Am. 2018;49(2):211-22. doi: 10.1016/j.ocl.2017.12.001.
4. Meena S, Sharma P, Sambharia AK, Dawar A. Fractures of distal radius: an overview. J Family Med Prim Care. 2014;3(4):325-32. doi: 10.4103/2249-4863.148101.
5. Christersson A, Nysjö J, Berglund L, et al. Comparison of 2D radiography and a semi-automatic CT-based 3D method for measuring change in dorsal angulation over time in distal radius fractures. Skeletal Radiol. 2016;45(6):763-9. doi: 10.1007/s00256-016-2350-6.
6. O'Malley MP, Rodner C, Ritting A, et al. Radiographic interpretation of distal radius fractures: visual estimations versus digital measuring techniques. Hand (N Y). 2014;9(4):488-93. doi: 10.1007/s11552-014-9666-2.
7. Baumbach SF, Binder J, Synek A, et al. Analysis of the three-dimensional anatomical variance of the distal radius using 3D shape models. BMC Med Imaging. 2017;17(1):23. doi: 10.1186/s12880-017-0193-9.
8. Gehweiler D, Teunis T, Varjas V, et al. Computerized anatomy of the distal radius and its relevance to volar plating, research, and teaching. Clin Anat. 2019;32(3):361-8. doi: 10.1002/ca.23320.
9. Suojärvi N, Tampio J, Lindfors N, Waris E. Computer-aided 3D analysis of anatomy and radiographic parameters of the distal radius. Clin Anat. 2021;34(4):574-80. doi: 10.1002/ca.23615.
10. Lindtner R, Kampik L, Putzer D, et al. Advancements in high-resolution computed tomography: revolutionising bone health micro-research. Bioengineering. 2025;12(11):1189. doi: 10.3390/bioengineering12111189.
11. Smees CJ, van Es EM, Tuijthof GJM, et al. Comparison of 3D CT and 2D radiograph measurements of the wrist in extra-articular malunited distal radius fractures. J Hand Surg Eur Vol. 2024;49(5):546-53. doi: 10.1177/17531934231213790.

12. Valerio T, Lupon E, Quemener-Tanguy A, et al. Morphometric and curvature CT-based study of the distal radius watershed line. Hand Surg Rehabil. 2025;44(4):102168. doi: 10.1016/j.hansur.2025.102168.
13. Shivdas S, Hashim MS, Ahmad TS. A three-dimensional virtual morphometry study of the sigmoid notch of the distal radius. J Orthop Surg (Hong Kong). 2018;26(3):2309499018802504. doi: 10.1177/2309499018802504.
14. Asai R, Ikumi A, Eda Y, et al. Relationship between physical characteristics and morphological features of the articular radius surface. Diagnostics. 2024;14(18):2005. doi: 10.3390/diagnostics14182005.
15. Eda Y, Asai R, Kohyama S, et al. Three-dimensional morphometric analysis of the volar cortical shape of the lunate facet of the distal radius. Diagnostics. 2024;14(16):1802. doi: 10.3390/diagnostics14161802.
16. Cho HJ, Kim S, Kwak DS. Morphological study of the anterior surface of the distal radius. Biomed Res Int. 2017;2017:8963768. doi: 10.1155/2017/8963768.
17. Oppermann J, Bredow J, Beyer F, et al. Distal radius: anatomical morphometric gender characteristics. Arch Orthop Trauma Surg. 2015;135(1):133-9. doi: 10.1007/s00402-014-2112-7.
18. Yoneda H, Iwatsuki K, Hara T, et al. Interindividual anatomical variations affect the plate-to-bone fit in distal radius fixation. J Orthop Res. 2016;34(6):953-60. doi: 10.1002/jor.23125.
19. Singh TS, Sadagatullah AN, Yusof AH. Morphology of distal radius curvatures: a CT-based study. Singapore Med J. 2015;56(10):562-6. doi: 10.11622/smedj.2015130.
20. Kumar A, Passey J, Chouhan D, et al. CT-based characterization of the volar surface of the distal radius. J Hand Surg Asian Pac Vol. 2021;26(1):77-83. doi: 10.1142/S2424835521500120.
21. Chiri W, MacLean SB, Clarnette J, et al. Anatomical and clinical concepts in distal radius volar ulnar corner fractures. J Wrist Surg. 2022;11(3):238-49. doi: 10.1055/s-0042-1748674.
22. Bain GI, MacLean SBM, McNaughton T, et al. Microstructure of the distal radius and its relevance to fractures. J Wrist Surg. 2017;6(4):307-15. doi: 10.1055/s-0037-1602849.
23. Cai XB, Lu ZH, Peng Z, et al. Neural network model for intelligent classification of distal radius fractures. Orthop Surg. 2025;17(5):1513-24. doi: 10.1111/os.70034.
24. Oura K, Otake Y, Shigi A, et al. Prediction of forearm bone shape using partial least squares regression. Int J Med Robot. 2017;13(3). doi: 10.1002/rcs.1807.
25. Baumbach SF, Binder J, Synek A, et al. Analysis of 3D anatomical variance of the distal radius. BMC Med Imaging. 2017;17(1):23. doi: 10.1186/s12880-017-0193-9.

Tables

Table 1. Summary of the performance of each regression model

Parameter	Model	R^2	RMSE	MAE
Linear distance	Polynomial	0.913	1.181 mm	0.943 mm
Linear distance	Polynominal with sex adjustment	0.917	1.154 mm	0.922 mm
Vertical distance	Polynomial	0.914	1.174 mm	0.933 mm
Vertical distance	Polynominal with sex adjustment	0.918	1.144 mm	0.909 mm
Palmar tilt	Polynomial	0.089	5.42°	4.14°
Palmar tilt	Polynominal with sex adjustment	0.091	5.41°	4.14°

Figures

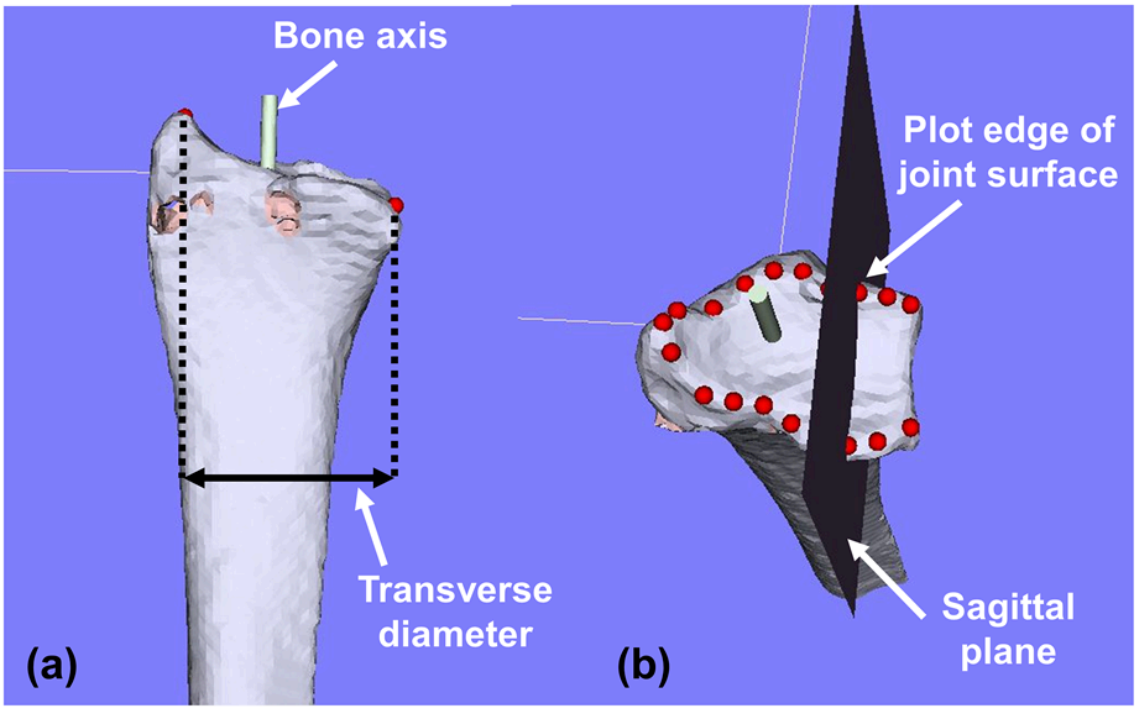


Figure 1

Figure 1

Definitions of transverse diameter and the dorsal and palmar reference points.

(a) Transverse diameter. The transverse diameter was measured as the vertical distance from the tip of the radial styloid to the ulnar margin in the coronal plane. (b) Reference points. Coordinates of dorsal and palmar reference points at the edge of distal radius joint surface were recorded at 3-mm intervals.

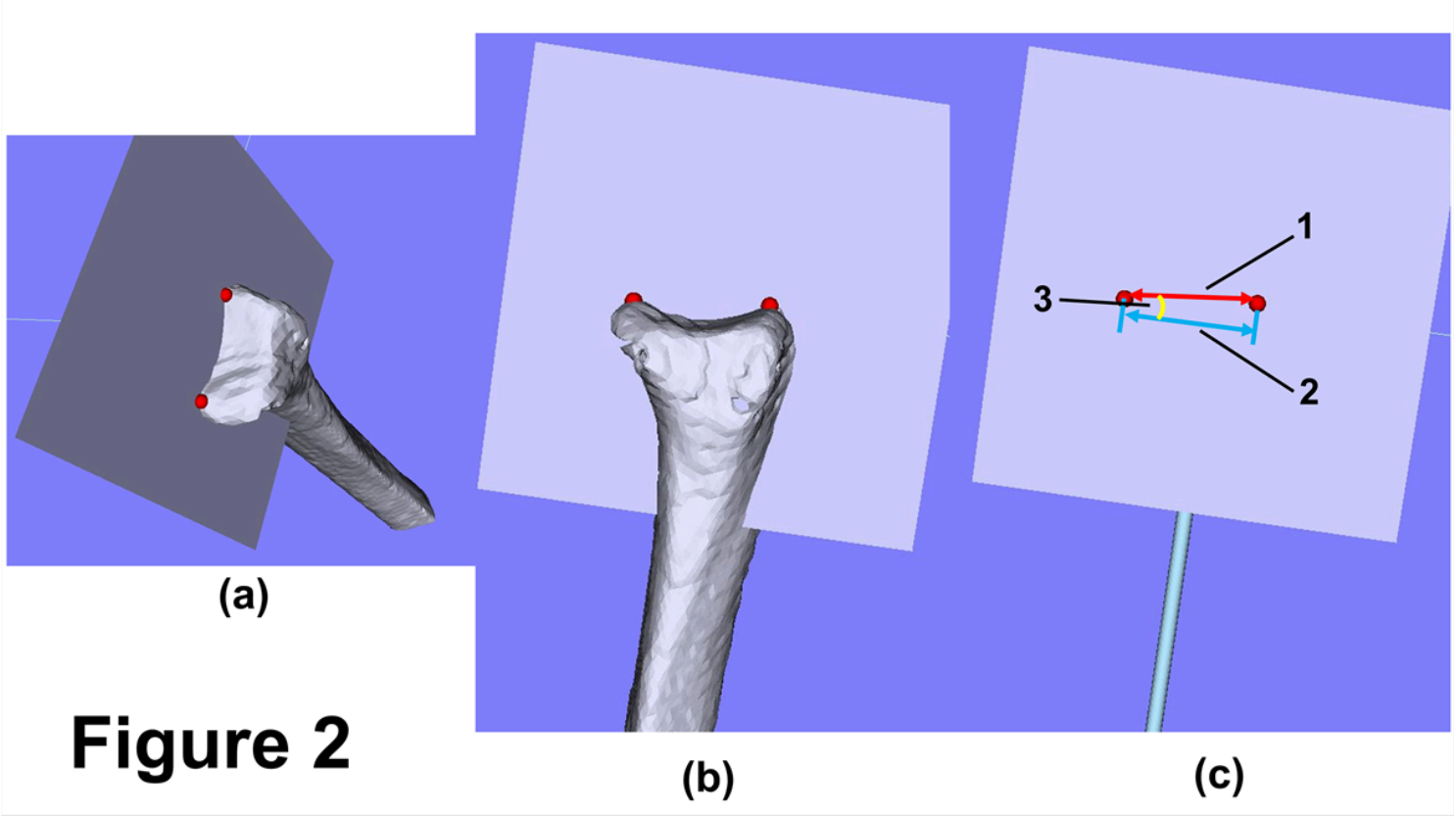


Figure 2

Measurements of linear distance, vertical distance, and palmar tilt on the sagittal plane.

(a) Sagittal reference planes were created at 3-mm intervals.

(b) Dorsal and palmar reference points at the edge of distal radius joint surface were plotted.

(c) Based on the 3D coordinate of the reference points, linear distance (1), vertical distance (2), and palmar tilt (3) were calculated.

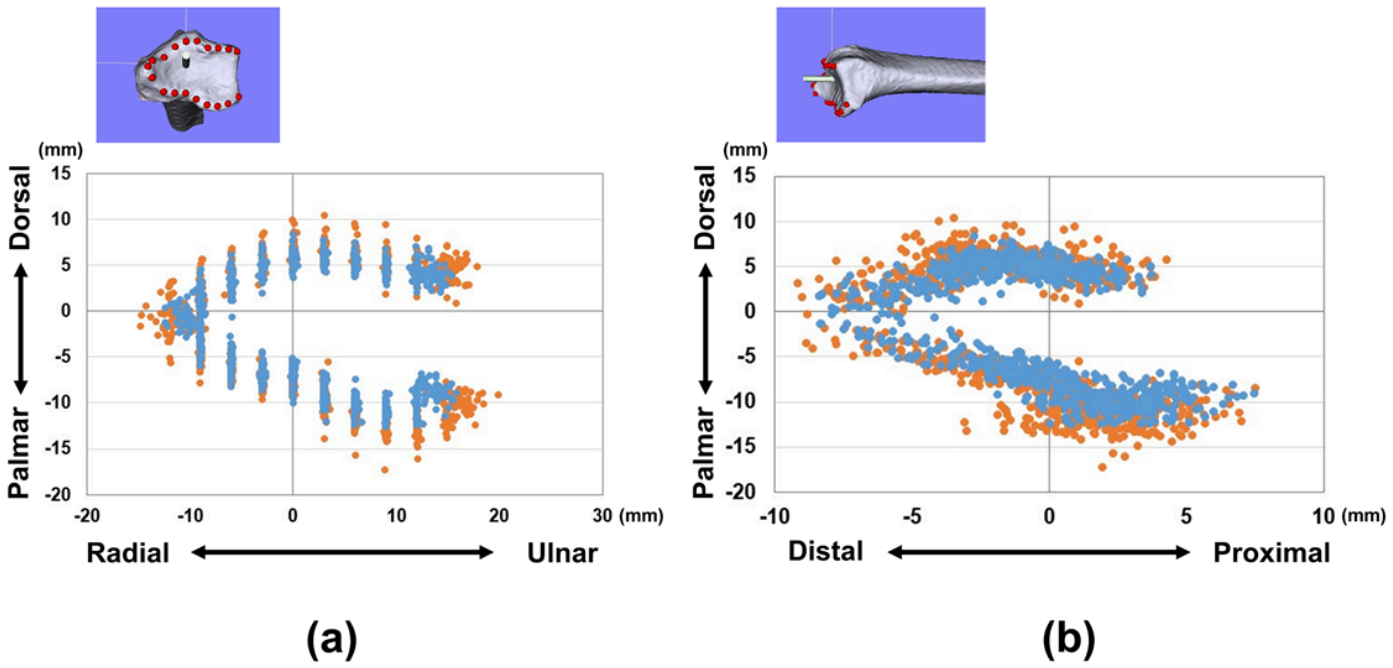


Figure 3

Figure 3

Actual plots on 2D coordinates.

(a) Axial plane. (b) Sagittal plane.

Blue dots indicate female data, and orange dots indicate male data.

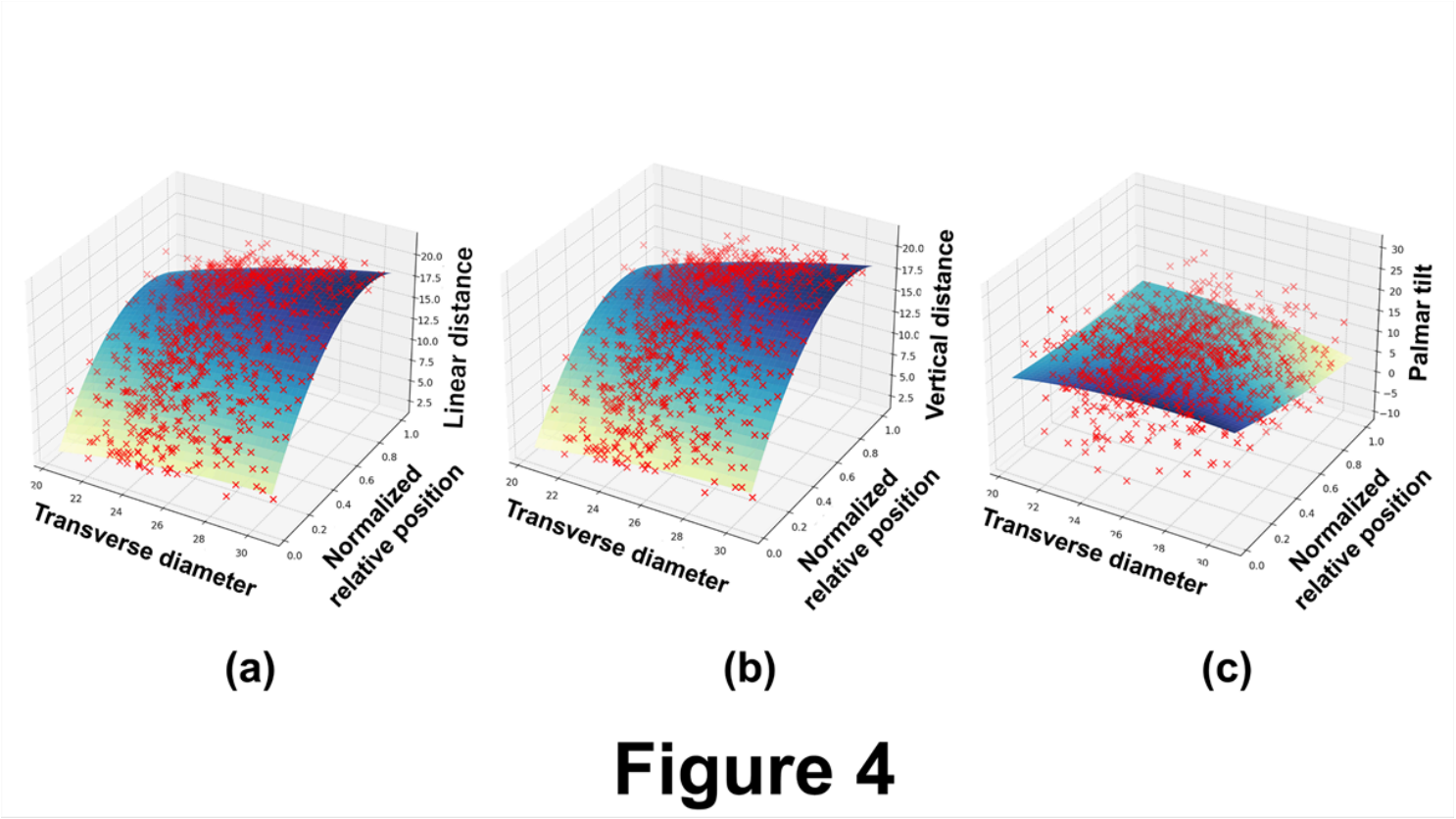


Figure 4

Figure 4

Results of 3D plots for each parameter.

(a) Linear distance. (b) Vertical distance. (c) Palmar tilt.

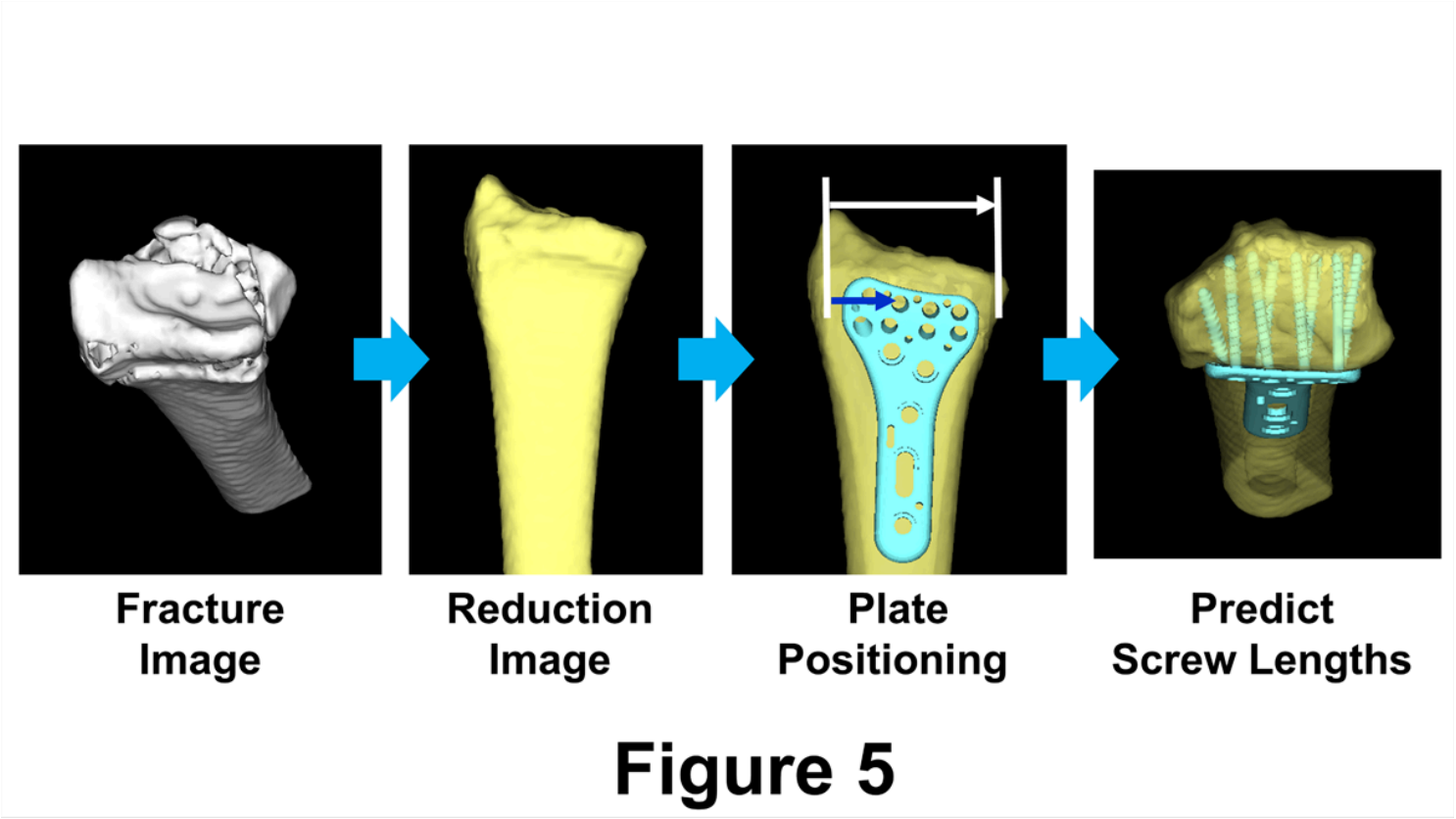


Figure 5

An example of clinical use for the regression model.

If the reduction and plate placement can be determined during preoperative planning, screw lengths can be automatically determined using the regression model.